

# Rapid tip-directed movement of Golgi equivalents in growing *Aspergillus nidulans* hyphae suggests a mechanism for delivery of growth-related materials

Michelle A. Hubbard and Susan G. W. Kaminskyj

Department of Biology, University of Saskatchewan, 112 Science Place, Saskatoon, SK S7N 5E2, Canada

## Correspondence

Susan G. W. Kaminskyj  
Susan.Kaminskyj@usask.ca

Golgi equivalents (GEs) process materials in the fungal secretory pathway. Despite the importance of localized secretion in fungal tip growth, GE behaviour in living hyphae has not been documented. The distribution was monitored of an *Aspergillus nidulans* putative GE-associated protein, CopA, tagged with GFP (CopA–GFP). This co-localized with a Golgi body/GE marker established in other systems,  $\alpha$ -2,6-sialyltransferase, tagged with red fluorescent protein (ST–RFP). CopA–GFP and ST–RFP distributions responded similarly to brefeldin A, which impairs Golgi/GE trafficking. We used a CopA–GFP, *hypA1* strain to study GE distribution and behaviour in growing *A. nidulans* hyphae. This strain has a wild-type phenotype at 28 °C, can be manipulated by changing growth temperature or by use of cytoskeleton inhibitors, and its GE behaviour is consistent with that in a wild-type-morphology strain. *A. nidulans* GEs were more abundant at hyphal tips than subapically, and showed saltatory motility in all directions. Anterograde GE movements predominated. These were positively correlated with, but at least 10-fold faster than, hyphal growth rate, under all growth and experimental conditions investigated. The actin inhibitor latrunculin B reduced both anterograde GE movement and hyphal growth rate, whereas the microtubule (MT) depolymerizer benomyl increased anterograde GE movement and decreased hyphal growth rate. The MT stabilizer taxol increased *A. nidulans* GE movement but not hyphal growth rate. *A. nidulans* GE motility appears to have a complex dependence on both actin and MTs. We present a model for apical delivery of growth materials in which *A. nidulans* GEs play a role in long-distance transport.

Received 7 November 2007

Revised 19 February 2008

Accepted 20 February 2008

## INTRODUCTION

Fungal tip growth uses the coordinated activities of the endomembrane and cytoskeletal systems to target growth materials to the hyphal apex (Bartnicki-Garcia, 2002; Heath, 1990, 1995). Golgi bodies process and sort materials (Farquhar & Palade, 1981, 1998; Matheson *et al.*, 2006; Mogelsvang & Howell, 2006), including those destined for secretion. Fungal Golgi equivalents (GEs) differ morphologically from Golgi bodies in animals and plants but perform similar functions (Beckett *et al.*, 1974; Bentivoglio & Mazzarello, 1998; Cole *et al.*, 2000), making them central players in the tip growth process. As in most fungi, *Aspergillus nidulans* GEs imaged with transmission electron microscopy (TEM) have single pleiomorphic cisternae (Beckett *et al.*, 1974; Kaminskyj & Boire, 2004; Kurtz *et al.*, 1994).

**Abbreviations:** BFA, brefeldin A; CaMV, cauliflower mosaic virus; GE, Golgi equivalent; MT, microtubule; RFP, red fluorescent protein; ST,  $\alpha$ -2,6-sialyltransferase; TEM, transmission electron microscopy.

A supplementary figure (video clip) showing Golgi equivalent motility in *Aspergillus nidulans* strain AAB1 is available with the online version of this paper.

The distribution of organelles (Bartnicki-Garcia, 2002) and proteins (McGoldrick *et al.*, 1995; Sharpless & Harris, 2002) can be used to infer their function. Evidence from *A. nidulans* (Breakspear *et al.*, 2007), *Aspergillus oryzae* (Akao *et al.*, 2006), *Candida albicans* (Rida *et al.*, 2006) and *Saccharomyces cerevisiae* (Matsuura-Tokita *et al.*, 2006) suggests that GE distribution in fungi is related to tip growth.

The behaviour of organelles in living *A. nidulans* hyphae has been revolutionized by fluorescent protein tagging (e.g. Suelmann & Fischer, 2000a, b). Such studies depend on verified localizations, using comparisons with independent localization methods. In *A. nidulans*, *sod<sup>VI</sup>C* (stabilization of disomy in chromosome VI) has been shown to encode a protein with high similarity to *Saccharomyces cerevisiae*  $\alpha$ COPI (Whittaker *et al.*, 1999). The COPI coat is required for one type of GE-derived vesicle formation (Bentivoglio & Mazzarello, 1998; Boevink *et al.*, 1998; Hawes & Satiat-Jeunemaitre, 2005). Breakspear *et al.* (2007), who renamed *sod<sup>VI</sup>C* as *copA*, showed that CopA–GFP localized to punctate arrays in *A. nidulans* hyphae. These arrays were adversely affected by brefeldin A (BFA) treatment, suggesting that they were *A. nidulans* GEs. Rat  $\alpha$ -2,6-sialyltransferase (ST)

contains a transmembrane domain that has been shown to be important for Golgi body retention in animals (Munro, 1991) and plants (Wee *et al.*, 1998), and for GE localization in yeast (Schwientek *et al.*, 1995), suggesting that it is a reliable marker with which to confirm the localization of CopA–GFP.

A. Breakspear and S. S. Assinder (University of Bangor, UK) provided us with a CopA–GFP strain in a *hypA1* temperature-sensitive background. The *hypA* gene encodes an orthologue of *Saccharomyces cerevisiae* Trs120p, a regulatory subunit in the COPII secretory pathway implicated in fungal GE transit (Shi *et al.*, 2004). When grown at 28 °C, *hypA1* strains have a wild-type phenotype (Kaminskyj & Hamer, 1998; Kaminskyj & Boire, 2004; Shi *et al.*, 2004). When grown at 42 °C, *hypA1* strains have reduced cell polarity, swollen GEs and thick cell walls, but these restrictive-phenotype cells establish wild-type-morphology hyphal branches within an hour of being shifted to 28 °C (Kaminskyj & Hamer, 1998; Kaminskyj & Boire, 2004; Shi *et al.*, 2004).

Here, we confirm the localization of CopA–GFP at GEs in growing *A. nidulans* hyphae by co-localization with the ST transmembrane domain tagged with red fluorescent protein (RFP). *A. nidulans* GEs showed saltatory motility, with movements being predominantly anterograde. We explored the relationship between the distribution and movement of *A. nidulans* GEs with respect to cell polarity and tip growth using the *hypA1* temperature-sensitive morphogenesis allele and cytoskeleton-targeting drugs. Our results suggest that long-distance delivery of growth-related materials to the hyphal tip may employ anterograde GE movements.

## METHODS

**A. *nidulans* strains and growth conditions.** The biological materials used in this study are listed in Table 1. Media and culture methods are described in Hubbard & Kaminskyj (2007) and

Kaminskyj (2001). Unless stated otherwise, all cells for all experiments were grown at 28 °C, and had a wild-type phenotype (Kaminskyj & Hamer, 1998). Most experiments used strain AAB1 with GFP under the control of the *alcA* promoter (Felenbok, 1991). GFP expression was induced by growth on complete medium (CM) containing 1% (v/v) glycerol or 1% ethanol as the sole carbohydrate source, or on Difco nutrient agar supplemented with 0.5% threonine. Anhydrous ethanol or solid threonine was added to cool, autoclaved media.

For microscopy, freshly harvested spores were inoculated onto sterile dialysis tubing overlying solid medium, and grown overnight at 28 °C (Hubbard & Kaminskyj, 2007). For drug-treated cells, the dialysis tubing and overlying hyphae were mounted in a microscope slide chamber in ~100 µl liquid medium that contained solvents and cytoskeleton-selective inhibitors as required, and allowed to recover for 30 min before observation, as described in Hubbard & Kaminskyj (2007). Mounting induced transient hyphal tip swelling, which made a convenient marker for identifying vigorously growing cells. Observations were terminated by 120 min.

Some hyphae were treated with BFA. In this case, hyphae were mounted in the slide chamber in CM-ethanol or nutrient broth-threonine and given 30 min for recovery, then medium plus BFA was added by rinsing through the slide chamber. Observations began as soon as possible following addition of BFA and were terminated after 60 min.

**Inhibitors.** Benomyl, paclitaxel (trade name, Taxol) and anhydrous DMSO were from Sigma. Latrunculin B (hereafter, latrunculin) was from Molecular Probes. All other chemicals were from VWR. Inhibitors were diluted from stock solutions with room-temperature liquid medium immediately before use.

Benomyl was stored at 4 °C as a 10 mg ml<sup>-1</sup> stock in 100% ethanol, and used at 1 µg ml<sup>-1</sup> in 0.01% ethanol. Latrunculin was stored as a 25 mg ml<sup>-1</sup> stock in 100% ethanol at -20 °C, and used at 5 µg ml<sup>-1</sup> in 0.2% ethanol. Taxol was stored at -20 °C as a 2 mM stock in 100% DMSO and used at 50 µM in 0.25% DMSO. DMSO was purchased as 1 ml ampoules of dry solvent, and the stock was stored over desiccant. BFA was stored at -20 °C as a 5 mg ml<sup>-1</sup> stock in 100% methanol, and used at 10 µg ml<sup>-1</sup> in 0.5% methanol. The inhibitor concentrations were similar to or lower than those typically used (benomyl, BFA and latrunculin), or were the lowest for which a response was detected (taxol) as described in Hubbard & Kaminskyj (2007).

**Confocal microscopy.** *A. nidulans* hyphae were imaged with a Zeiss META 510 laser scanning confocal microscope with a Plan

**Table 1.** Strains and plasmids used in this study

Strain or plasmid	Relevant characteristics
<b><i>A. nidulans</i> strains</b>	
AAB1*	AlcA-CopA-GFP; <i>hypA1</i> , <i>pabaA6</i> ; <i>veA1</i>
AMH1†	AlcA-CopA-GFP, <i>paba A6</i> , <i>γA2</i> ; <i>pyrG89</i> ; <i>veA1</i>
AMH2‡	AlcA-CopA-GFP; CaMV 35S-RFP-4,6-ST; <i>paba A6</i> , <i>γA2</i> ; <i>pyrG89</i> :: <i>N. crassa pyr4</i> <sup>+</sup> , <i>veA1</i>
<b>Plasmids</b>	
ARp1‡	Autonomously replicating AMA1 plasmid, amp <sup>R</sup> , containing <i>N. crassa pyr4</i> <sup>+</sup> as a selectable marker
ST-RFP§	CaMV 35S-RFP-ST, amp <sup>R</sup>

\*A gift from Susan Assinder and Andrew Breakspear (University of Wales, Bangor, UK).

†This study.

‡Shi *et al.* (2004).

§A gift from Chris Hawes (Oxford Brookes University, Oxford, UK) and Federica Brandizzi (University of Saskatchewan, SK).

Apochromat  $\times 63$ , numerical aperture 1.2 multi-immersion objective equipped with phase-contrast optics. CopA–GFP imaging used 488 nm excitation, 5–10% power from an argon multispectral laser operated at 5.9 A, with emission controlled by a BP505-530 filter. ST–RFP imaging used 543 nm excitation, 5–10% power from a 25 mW HeNe1 laser, with emission controlled by an LP585 filter. For each type of imaging, eight or 16 scans at 0.6–2.5  $\mu\text{s}$  per pixel were used to improve signal to noise ratio. Optical sections were 1.2  $\mu\text{m}$  thick, and chosen to be near-median focal level, as judged by cell profile. Observations were based on single optical sections taken from time-lapse series, 5–20 images collected over 60–300 s. Fluorescence images for studying GE movement and transmitted images for hyphal growth rate were collected at the same time.

Hyphae were chosen for analysis if they were located at the colony margin, had an even width profile, had a smoothly tapered tip and had grown out from the characteristic mounting-induced morphology, that is, a swollen tip or an abrupt change in growth direction. Hyphae that had not responded in this way to mounting were assumed to be non-growing and were not selected for analysis. However, whether a particular hypha was actually growing, and at what rate, was not determined until after the data were collected.

**A. nidulans containing RFP-tagged ST.** A 52 aa transmembrane domain from rat ST (Munro, 1991), tagged at the C terminus with monomeric red fluorescent protein (mRFP, hereafter RFP) under the control of the cauliflower mosaic virus (CaMV) 35S promoter was provided by F. Brandizzi (formerly University of Saskatchewan) and C. Hawes (Oxford Brookes University). *A. nidulans* strain AMH1 was transformed using 4  $\mu\text{g}$  ST–RFP DNA plus 1  $\mu\text{g}$  ARp1–*pyr4* DNA, which contains *Neurospora crassa pyr4<sup>+</sup>* as a selectable marker, following the procedure described in Shi *et al.* (2004). Transformants were grown at 28 °C for 72 h before colonies were tested for expression of RFP and GFP fluorescence. Strain AMH2 expressed RFP on all growth media, and expressed GFP on CM-ethanol or nutrient broth-threonine. GFP and RFP expression were probed on Western blots of AAB1 and AMH2 grown under *AlcA*-inducing and -suppressing conditions, respectively, and using a polyclonal anti-GFP that can recognize both GFP and RFP [Santa Cruz Biotechnology Inc. (SCBI) Technical Support, personal communication]. Both constructs had bands with the expected mobility, and in addition CopA–GFP had some free GFP (see figure 3-3 in Hubbard, 2007) that likely contributed to background fluorescence.

**Statistical and graphical analysis.** Data are expressed as the mean  $\pm$  SEM. Statistical analyses used the 2000 version of Microsoft Excel with data analysis add-ins, which generates probability values. Statistical comparisons between treatments used one-way, single-factor ANOVA, and post-hoc comparisons used Fisher predicted least-square difference (PLSD). Numerical data are presented using the 2000 version of Microsoft Excel. Images are presented using Adobe Photoshop 7.0 with minor contrast adjustments.

## RESULTS

### GE distribution in *A. nidulans* hyphae

In living *A. nidulans* hyphae, both the ST–RFP and CopA–GFP markers had punctate localizations consistent with that expected for GEs (Fig. 1a, b). These were roughly 0.5–1  $\mu\text{m}$  in diameter, and co-localized extensively (Fig. 1c). The CopA–GFP pattern had a somewhat coarse cytoplasmic background, consistent with COPI-coated vesicles that cannot be resolved by confocal fluorescence. Comparing fluorescence and transmitted images (Fig. 1c, d) at least

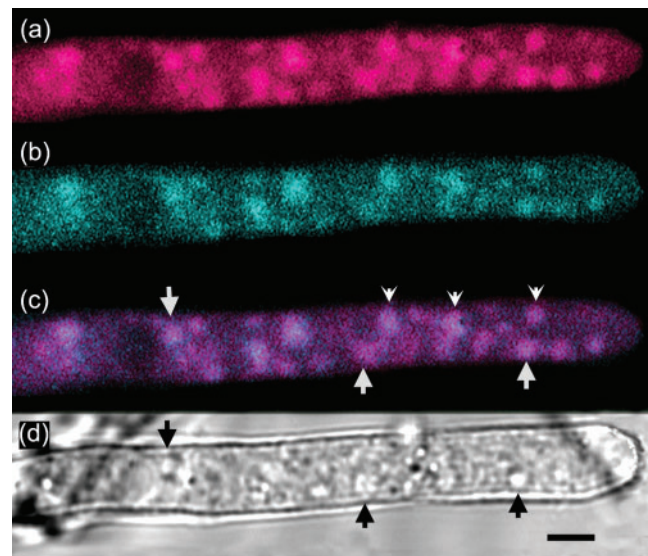


**Fig. 1.** Distributions of fluorescent protein-tagged GE markers in a wild-type-phenotype *A. nidulans* hypha show extensive co-localization when viewed with confocal microscopy in a near-median section. (a) Distribution of the transmembrane domain of ST, C-terminal tagged with RFP (ST–RFP), pseudo-coloured magenta. (b) Distribution of CopA, C-terminal tagged with GFP, pseudo-coloured cyan. (c) Colocalization of (a) and (b). (d) Transmitted light image. Arrows in (c) and (d) indicate punctate fluorescence in (c) that appears to co-localize with inclusions in the transmitted image in (d). Arrowheads in (c) indicate punctate fluorescence in (c) that lacks such apparent co-localization. Bar, 2  $\mu\text{m}$ .

seven of 26 large fluorescent structures appeared to co-localize with cytoplasmic structures of a similar size that were visualized with transmitted light (arrows), although many others did not (arrowheads). Epifluorescence images viewed with confocal optics have a shallower depth of focus than their associated transmitted light images, which makes precise spatial correlations difficult. Nevertheless, this is intriguing, since GEs have not, to our knowledge, been imaged previously without staining in living fungal cells.

BFA affects endomembrane trafficking by inhibiting an early stage in COPI vesicle formation. *A. nidulans* hyphae treated with 10  $\mu\text{g}$  BFA  $\text{ml}^{-1}$  had less well-defined GE patterns following 25 min of treatment (Fig. 2a–d) which is consistent with the anticipated BFA effect. After 60 min of BFA treatment there were preliminary indications of a reticulate network (arrows in Fig. 2e) that was entirely unlike the punctate arrays seen in untreated cells.

In wild-type-morphology *A. nidulans* hyphae, GEs were significantly more abundant in the apical 25  $\mu\text{m}$  than further back ( $P < 0.01$ , ANOVA). This apical region had one or two GE per micrometre of hyphal length. In more subapical regions GE abundance was about half that near the tip, and this lower level persisted for tens of micrometres. In cells with the *hypA1* restrictive phenotype,

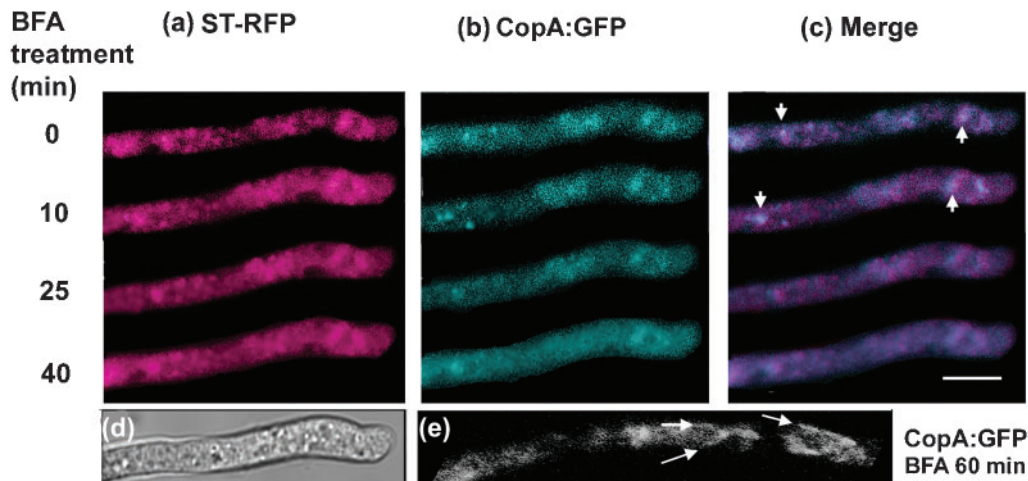


**Fig. 2.** Effect of BFA on fluorescent protein-tagged GE marker distributions in a wild-type-morphology *A. nidulans* hypha. The numbers indicate the time in minutes since the beginning of BFA treatment, which inhibited tip growth. (a) The GE transmembrane marker ST-RFP (magenta) and (b) CopA-GFP (cyan) have predominantly punctate localizations prior to BFA treatment. (c) Merged images of ST-RFP and CopA-GFP. Arrowheads indicate GEs, the appearance of which became more diffuse following BFA treatment. (d) Transmitted light image of the hypha in (a–c) corresponding to the 40 min BFA treatment. The distribution of both ST-RFP and CopA-GFP became more diffuse within 25 min of treatment. (e) Hypha treated with BFA and imaged for CopA-GFP after 60 min, showing development of putative reticulate labelling patterns (arrows) that were unlike the patterns at 0–10 min. Bar in (c), 5  $\mu$ m for all parts.

the growing tip was tapered and clearly distinguishable from the rounded spore-end of the germling. In *hypA1* restrictive-phenotype cells, the region of high GE abundance was clearly at the growing tip end.

### ***A. nidulans* GEs are mobile, independent of tip growth**

*A. nidulans* GEs were mobile within the near-apical cytoplasm, showing randomly directed saltatory movements. Some individual GEs could be tracked between frames of time-lapse series of single near-median optical sections, and were found to move independently in all directions (see Supplementary Fig. S1). We defined GE movements as anterograde, retrograde or lateral (Fig. 3a), by comparing their positions between sequential frames. Transmitted light images were used to measure growth rate after the series were collected. GE motion was faster in growing hyphae, and tended to be anterograde (Fig. 3c). Rates were similar in strains with wild-type (AMH1, AMH2) and *hypA1* (AAB1) backgrounds grown at 28 °C. GE movements were examined in repolarizing *hypA1* cells, which had been grown for 14 h at 42 °C (at which temperature they form viable but poorly polarized cells) and then shifted to 28 °C. Under these conditions, new branches visible with transmitted light formed within 1 h (Fig. 3b). These would later grow into wild-type-morphology hyphae.

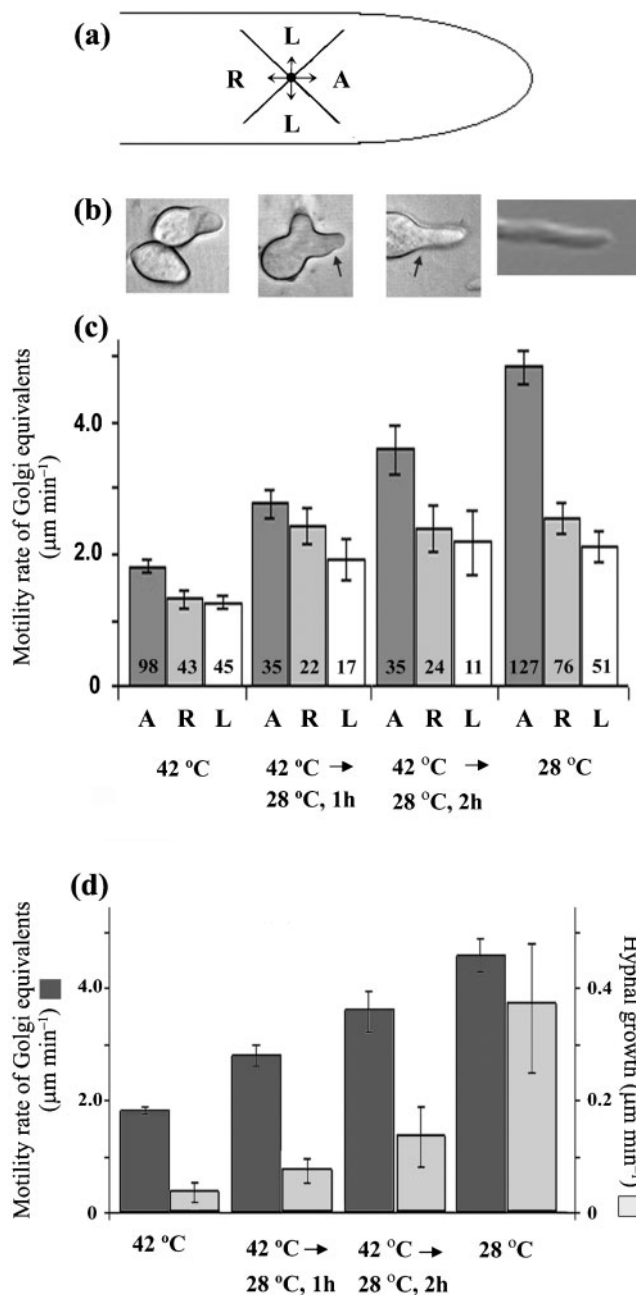
In repolarizing *hypA1* phenotype cells, anterograde GE movements were about twice as fast (Fig. 3c) and twice as

frequent (Fig. 3c) as those in other directions. Rates of anterograde GE movement were most different between poorly (grown at 42 °C) and highly polarized (grown at 28 °C) cells. There was a clear trend towards an increasing rate of anterograde movement during repolarization (Fig. 3c), but not towards retrograde and lateral movements (Fig. 3b) over the same time-course. Since anterograde GE movements seem intuitively to be the most immediately relevant to tip growth, the remaining data will focus on these.

Fig. 3(d) compares tip growth rates and anterograde GE movement rates in *hypA1* cells growing at permissive and restrictive temperatures, and during cell repolarization, a more detailed analysis of the anterograde data shown in Fig. 3(c). The average anterograde GE movement rate was always at least tenfold faster than growth rate. In other words, there was a net anterograde movement of GEs (Fig. 3d), consistent with delivery of growth-related materials to the cell tip.

### **Cytoskeletal involvement in *A. nidulans* GE movements**

GE movement will depend on the actin or microtubule (MT) cytoskeletons, or on both. We treated *A. nidulans* hyphae with actin-depolymerizing (latrunculin), or MT-depolymerizing (benomyl) or -stabilizing (taxol) drugs to study the relative effects on GE movements. The final drug concentrations were prepared from concentrated stock solutions in solvent, so we compared drug effects with



those for solvent-treated control cells. Preliminary studies comparing GE movement and hyphal growth rates for strain AAB1 growing on CM-ethanol, CM-glycerol and nutrient broth-threonine showed no significant difference in GE movement or hyphal growth rate between different growth media (Fig. 4a; data not shown).

Hyphae treated with 5 mg latrunculin  $\text{ml}^{-1}$  had a minimal rate of tip growth (Fig. 4b), consistent with the importance of an intact actin cytoskeleton for many cellular processes. Anterograde GE movement in latrunculin-treated cells was significantly reduced compared with controls, but was not abolished (Fig. 4b). Hyphae treated with 1  $\mu\text{g}$  benomyl  $\text{ml}^{-1}$ , which we had shown previously depolymerizes

**Fig. 3.** Direction and speed of motion of *A. nidulans* GEs, localized with CopA-GFP, in 42 °C-grown *hypA1* restrictive-phenotype cells that were allowed to repolarize following a shift to 28 °C. (a) Direction of GE movement with respect to the hyphal tip: anterograde (A), retrograde (R) or lateral (L), as described in Methods. (b) Photomicrographs showing representative morphologies of *hypA1* and repolarizing phenotypes. The arrows indicate new growth following a shift from 42 to 28 °C. GE movement is shown in repolarizing *A. nidulans hypA1* cells, which produce wild-type branches (arrows indicate the growth transition associated with the shift from 42 to 28 °C). (c) GE motility in *hypA1* restrictive and repolarizing *A. nidulans* AAB1 cells. Spores were grown for 14 h at 42 °C. For the repolarizing phenotypes, AAB1 spores were grown at 42 °C for 14 h, then shifted to 28 °C for 1 or 2 h. For the permissive phenotype, AAB1 spores were grown at 28 °C. Bars indicate rate of GE movement  $\pm$  SEM for each direction, with the numbers indicating the total number of GEs analysed from five cells. GE movement was predominantly anterograde, and was significantly faster than movement in other directions. (d) Anterograde GE movement (dark-grey bars) compared with tip growth rate (light-grey bars) for the cells shown in (c) was always at least 10-fold higher than the growth rate; note that the y-axis scales are 10-fold different. Both GE movement and growth rates increased significantly during cell repolarization. Error bars show SEM.

all cytoplasmic MTs within 2 min but does not prevent hyphal tip growth within 1 h (Hubbard & Kaminskyj, 2007), had reduced tip growth rates, but significantly increased anterograde GE movement (Fig. 4b). Hyphae treated with 50  $\mu\text{M}$  taxol, which we had shown previously significantly increases cytoplasmic MT abundance (Hubbard & Kaminskyj, 2007), significantly increased anterograde GE movement rate, but without increasing hyphal growth rate (Fig. 4c). All these drugs caused hyphal morphological abnormalities after several hours; however, we collected growth and GE data only within the first 1 h (benomyl) or 2 h (latrunculin and taxol) of treatment.

## DISCUSSION

This is believed to be the first study of GE localization, distribution and behaviour in living *A. nidulans* hyphae. CopA-GFP and ST-RFP localizations were typically round in optical section, but occasionally appeared to be oval or horseshoe-shaped (see figure 3-2 in Hubbard, 2007). These were consistent with *Aspergillus* GEs imaged with TEM, which have single pleiomorphic cisternae (Beckett *et al.*, 1974; Kaminskyj & Boire, 2004; Kurtz *et al.*, 1994), similar to those of *Pisolithus* (Xu *et al.*, 2004) and *Schizophyllum* (Rupeš *et al.*, 1995). Fluorescent structures are luminous, which enhances detection and can increase apparent size (Hubbard & Kaminskyj, 2007). The apparent size of *A. nidulans* GEs is also consistent with results from plants, which have numerous, motile Golgi bodies (Boevink *et al.*, 1998).

The CaMV promoter has been shown to induce gene expression in plants (Jefferson *et al.*, 1987; Odell & Nagy,

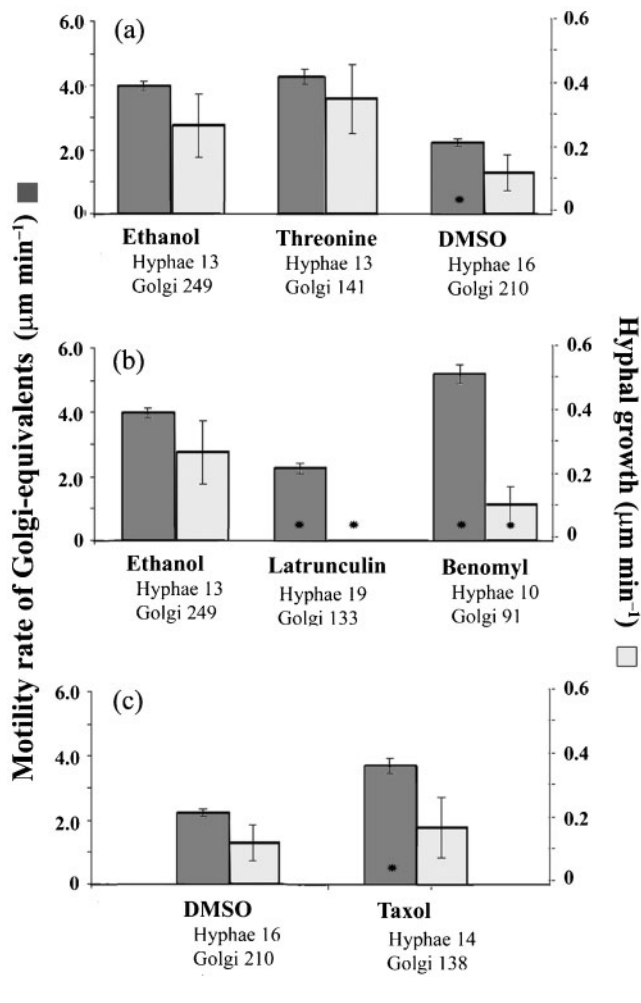


**Fig. 4.** Effect of solvents and cytoskeleton-inhibitory drugs on anterograde GE movement (dark-grey bars) and hyphal growth rates (light-grey bars) in wild-type-phenotype *A. nidulans* hyphae of strain AAB1 grown at 28 °C. Error bars show SEM. The rate of anterograde GE movement was always at least 10-fold higher than the growth rate in the same cells; note that the *y*-axis scales are 10-fold different. Retrograde and lateral movements were not significantly affected. Asterisks indicate a significant change compared with the respective control ( $P < 0.05$ , ANOVA). (a) Effect of the *AlcA* inducers 1.0% ethanol and 0.5% threonine, and of 0.25% DMSO in 1.0% ethanol. The rates of GE movement and growth were similar for ethanol and threonine, but DMSO caused a significant reduction in GE movement but not growth rate. (b) Effect of 5 µg latrunculin B ml<sup>-1</sup> and 1 µg benomyl ml<sup>-1</sup>, which target actin and MTs, respectively. Latrunculin treatment significantly reduced both GE movement and growth rate, whereas benomyl treatment increased GE motility while reducing growth rate. (c) Effect of 50 µM taxol in 0.25% DMSO. Compared with the control treatment, taxol significantly increased GE anterograde movement rate without increasing hyphal growth rate.

1985; Wee *et al.*, 1998) and in fungal species, including *S. cerevisiae* (Hirt *et al.*, 1990), *Uromyces appendiculatus* (Li *et al.*, 1993), *Ganoderma lucidum* and *Pleurotus citrinopileatus*

(Sun *et al.*, 2002), and *Pleurotus ostreatus* (Xu *et al.*, 2004). This is, to our knowledge, the first demonstration of its efficacy in *A. nidulans*.

The transmembrane domain of ST has been shown to be associated with Golgi bodies in animal (Munro, 1991), plant (Wee *et al.*, 1998) and fungal (Schwientek *et al.*, 1995) systems. This is, to our knowledge, the first demonstration of its localization in *A. nidulans*, in which the ST-RFP fluorescence labelling pattern was clearly consistent with that of CopA-GFP labelling. Thus, ST-RFP is likely to be useful for tracking *A. nidulans* GEs in order to examine their behaviour in living cells without the pharmacological effects noted previously with fluorescent BFA labelling in *Pisolithus* (Cole *et al.*, 2000), *Pleurotus* (Xu *et al.*, 2004) and *Schizophyllum* (Rupeš *et al.*, 1995).

The effect of BFA on CopA-GFP fluorescence distribution in living hyphae was consistent with that shown in Breakspear *et al.* (2007), and with changes seen with ST-RFP. BFA blocks the function of a Sec7 guanine nucleotide exchange factor (Donaldson *et al.*, 1992), which is required early in COPI coat formation (Helms & Rothman, 1992). Within 25 min of applying BFA, both the ST-RFP and CopA-GFP patterns became less distinct, as expected, since BFA dissociates COPI from vesicles and later affects GE morphology by perturbing vesicle trafficking (Jackson & Casanova, 2000). Khalaj *et al.* (2001) showed that 100 µg BFA ml<sup>-1</sup> induces perinuclear endomembrane redistributions in *Aspergillus niger* after 2 h. Our milder and shorter BFA treatments had less extreme effects, but were consistent with more dramatic redistributions over longer timescales.

### Distribution and motility of *A. nidulans* GEs

Most cellular constituents (turgor being a notable exception) show a tip-high gradient of abundance in growing hyphae, although the length and steepness of the individual gradients vary (Heath & Kaminskyj, 1989). Organelle distributions can be altered by cytoplasmic contractions during chemical fixation (Kaminskyj *et al.*, 1992), so we examined GE distributions in living *A. nidulans* hyphae. In near-median optical sections, fluorescence-localized GE populations were similar to those shown elsewhere with freeze-substitution TEM (Kurtz *et al.*, 1994). In addition, Breakspear *et al.* (2007) showed a similar GE abundance pattern in fixed hyphae. *A. nidulans* GEs are appropriately distributed to contribute to apical growth, being relatively more abundant in the near-apical cytoplasm.

In growing hyphae, the near-apical cytoplasm appears to move as a unit (sometimes called bulk flow) with respect to the lateral hyphal walls, using actin-dependent processes (Heath, 1990, 1995; Kaminskyj & Heath, 1996). Within the cytoplasm, independent nuclear (Morris *et al.*, 1995; Suelmann & Fischer, 2000b) and mitochondrial (Suelmann & Fischer, 2000a) movements are generated by cytoskeleton-dependent processes. When cytoskeletal function was

perturbed by benomyl, latrunculin or taxol, there was a trend for GEs to become relatively more concentrated near hyphal tips (data not shown), also seen in Breakspear *et al.* (2007) following nocodazole treatment. This is consistent with a tendency for cytoplasm to contract toward the apex following cytoplasm perturbation (Kaminskyj *et al.*, 1992; Kaminskyj & Heath, 1996).

The GE distribution pattern in *Aspergillus* correlates with that of cytoplasmic MTs, which is circumstantial evidence suggesting that longitudinal (but perhaps not lateral) GE motility could use MT-dependent motors. However, unexpectedly, both cytoplasmic MT depolymerization with benomyl and MT polymerization with taxol increased anterograde GE motility. Breakspear *et al.* (2007) showed that the *nudA1<sup>ts</sup>* cytoplasmic dynein heavy chain mutation does not affect GE positioning at restrictive temperature, despite substantial effects on nuclear positioning, suggesting that nuclear and GE motility are differently regulated.

In contrast to their lack of dependence on MTs, *Aspergillus* GE movement and tip growth are exquisitely dependent on the actin cytoskeleton. Actin-dependent motility has also been shown for plant Golgi bodies (Boevink *et al.*, 1998). *A. nidulans* hyphae treated for more than 2 h with any of these cytoskeleton-targeting drugs began to develop morphological abnormalities (Hubbard, 2007; Hubbard & Kaminskyj, 2007), suggesting that wall deposition and cell extension can continue despite sublethal cytoskeletal impairment, albeit with aberrant apical targeting. Clearly, the mechanisms underlying GE motility will prove to be complex.

### Anterograde transport of tip growth-related materials

Given the size of an *A. nidulans* wall vesicle (~50 nm diameter) and the area of cell membrane required for a growth rate of about 0.5  $\mu\text{m min}^{-1}$  (Hubbard & Kaminskyj, 2007) of a hypha about 3  $\mu\text{m}$  in diameter (Kaminskyj & Hamer, 1998), at least 600 vesicles per minute must fuse at the hyphal tip. If long-distance anterograde transport of growth-related materials in *Aspergillus* was in vesicles, then vesicle abundance should be relatively consistent in near-apical cytoplasm. However, TEM shows that *Aspergillus* hyphae have a substantially larger vesicle population in the apical 2–3  $\mu\text{m}$  compared with even a few micrometres slightly further back (see figure 4a in Kurtz *et al.*, 1994). Thus, long-distance wall material transport in vesicles is not consistent with vesicle distribution patterns in *Aspergillus* hyphae. This is unlike *Saprolegnia ferax*, where individual wall vesicles produced by Golgi bodies located in the central cytoplasm appear to migrate to and then be transported along the cell periphery (Heath & Kaminskyj, 1989). Fungal and oomycete hyphae have similar shapes, and the organisms have comparable lifestyles, but they are phylogenetically distant.

There are about 15 cytoplasmic MTs or MT bundles in the apical 20  $\mu\text{m}$  of an *A. nidulans* hypha (Hubbard &

Kaminskyj, 2007). If *A. nidulans* growth materials were transported in vesicles, along MTs, vesicle distributions visualized with electron tomography should be spatially correlated with cytoplasmic MTs. However, figure 2 in Hohmann-Marriott *et al.* (2006) does not provide support for this relationship. In addition, the average separation between vesicles and MTs is about 50 nm, twice the length expected for cytoplasmic dynein (R. Roberson, personal communication). Vesicle distribution in *Aspergillus* hyphae does not appear to be spatially correlated with cytoplasmic MTs, arguing against a direct role for MTs in vesicle motility.

It has generally been assumed that wall-forming materials in filamentous fungi are transported to hyphal tips in vesicles, by means of cytoplasmic MT-dependent motors (Bartnicki-Garcia, 2002; Breakspear *et al.*, 2007; Fischer & Veith, 2007). However, direct evidence to support this model is sparse, or argues to the contrary (Hohmann-Marriott *et al.*, 2006). Results described in Hubbard & Kaminskyj (2007) suggest that tip growth rates in *A. nidulans* are not quantitatively related to cytoplasmic MT number. Vesicle transport could also be mediated by actin, which has multiple roles in tip growth (Bartnicki-Garcia, 2002; Harris *et al.*, 1994; Heath, 1990, 1995; Kaminskyj & Heath, 1996). The mechanisms underlying organelle movement in *A. nidulans* have not been explored, apart from those of MTs in nuclear (Morris *et al.*, 1995; Suelmann & Fischer, 2000b) and actin in mitochondrial motility (Suelmann & Fischer, 2000a). Our data showing that *A. nidulans* GEs have predominant anterograde motility at rates far exceeding the rate of tip growth in the same cells suggest that growth-related materials might be transported to the tip packaged in GEs.

In contrast to a model proposing long-distance transport of wall vesicles in *A. nidulans*, the pattern of tip-localized vesicle abundance in *Aspergillus* hyphal tips is complementary to that of *Aspergillus* GEs (Kurtz *et al.*, 1994; Breakspear *et al.*, 2007; this paper). This then is consistent with the notion that GEs offload their contents in the vicinity of the Spitzenkörper, presumably as vesicles, prior to changes that permit them to fuse at the hyphal apex. In *A. nidulans* hyphae examined following diverse treatments, anterograde GE movement was consistently at least 10-fold faster than tip growth rates. This suggests that GEs may be delivering wall-building materials to near-apical regions of the hypha, potentially supplementing (or supplanting?) bulk delivery by individual vesicles.

### A model for the role of GE movement in *A. nidulans* tip growth

The model shown in Fig. 5 concerns the role of GE motility in *A. nidulans* hyphal growth. As discussed earlier, fungal GEs have a function analogous to that of Golgi bodies in animals and plants. Endoplasmic reticulum (ER) to GE transport in fungi (Fig. 5a) might occur at specialized sites, as has been proposed for yeasts (Bevis *et al.*, 2002;

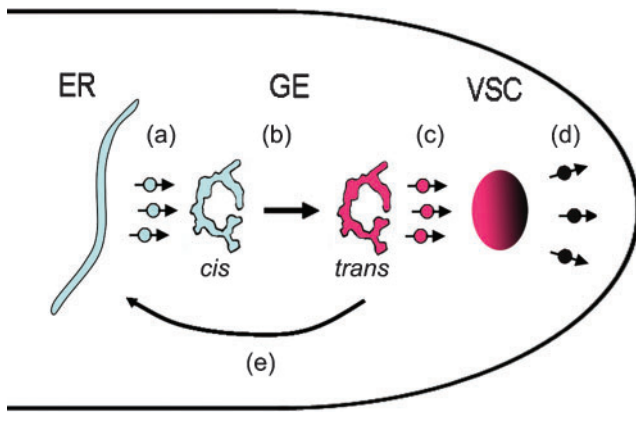


**Fig. 5.** Model describing how anterograde GE movement might contribute to hyphal tip growth. *Aspergillus* GEs are single pleiomorphic cisternae; this cartoon was adapted from a freeze-substitution transmission electron micrograph (see figure 4a in Kurtz *et al.*, 1994). (a) Endoplasmic reticulum (ER) to GE transport. GEs are transported toward the hyphal tip (b) at rates roughly 10-fold higher than that of tip growth. Maturation of *cis*-Golgi to *trans*-Golgi (indicated by colour change) may occur during anterograde transport. GEs do not accumulate at the hyphal tip because they unload their cargo (c) near the Spitzenkörper (vesicular supply centre; VSC). Changes in vesicle membranes associated with the VSC (indicated by colour gradient; individual vesicles are not shown) permit them to fuse with the cell membrane for secretion at the hyphal tip (d). Currently it is unclear whether the Golgi are disassembled or recycled following unloading. If GEs that have unloaded their cargo are recycled to subapical regions to collect more cargo, this could comprise a portion of the lateral or retrograde GE motility (e). Stages (a) and (c) and transit from the VSC to the cell membrane are depicted as being predominantly mediated by vesicle traffic, although direct ER–GE transport by transfer ER has been postulated for plants and certain yeasts.

Mogelsvang *et al.*, 2003) and plants (daSilva *et al.*, 2004; Matheson *et al.*, 2006). Both the ER (Fernández-Ábalos *et al.*, 1998; Maruyama & Kitamoto, 2007) and GEs (this paper; Breakspear *et al.*, 2007) are widely distributed in the apical cytoplasm of *A. nidulans* hyphae. Anterograde GE transport may be accompanied by maturation from *cis*-like to *trans*-like GE elements (Fig. 5b), a functional analogy to cisternal maturation in Golgi bodies, consistent with changes recently documented in yeast (Losev *et al.*, 2006; Matsuura-Tokita *et al.*, 2006). Despite predominantly anterograde GE movement, GEs do not accumulate at the tips of *A. nidulans* hyphae. Indeed, GEs were notably less abundant within 5  $\mu\text{m}$  of the tip, suggesting that they offload their cargo (Fig. 5c), presumably as vesicles destined for the Spitzenkörper (vesicle supply centre; VSC). VSC- and exocytosis-related events (Fig. 5d) are shown for completeness, but are not directly addressed by this model. Following unloading, GEs might be transported subapically to acquire more growth-related materials (Fig. 5e), which could account for at least some retrograde and lateral movements. Studies to investigate the events

involved in the loading, transport and unloading of GEs are under way.

## ACKNOWLEDGEMENTS

This research was supported by a Natural Sciences and Engineering Research Council (NSERC) grant to S.G.W.K., which is gratefully acknowledged. M.A.H. was supported by a University of Saskatchewan Dean's Graduate Scholarship and an NSERC Canada Graduate Scholarship (Masters). The Canada Foundation for Innovation is acknowledged for purchase of the Zeiss META510 confocal microscope. The Brandizzi (formerly University of Saskatchewan) and Hawes (Oxford Brookes University) groups supplied the ST–RFP plasmid. The Assinder group (University of Wales, Bangor, UK) provided the CopA–GFP, *hypA1* strain. We thank Xiaohui Bao for translating Xu *et al.* (2004), and anonymous reviewers for useful comments.

## REFERENCES

- Akao, T., Yamaguchi, M., Yahara, A., Yoshiuchi, K., Fujita, H., Yamada, O., Akita, O., Ohmachi, T., Asada, Y. & Yoshida, T. (2006). Cloning and expression of 1,2- $\alpha$ -mannosidase gene (*fmanIB*) from filamentous fungus *Aspergillus oryzae*: *in vivo* visualization of the FmanIBp–GFP fusion protein. *Biosci Biotechnol Biochem* **70**, 471–479.
- Bartnicki-Garcia, S. (2002). Hyphal tip growth: outstanding questions. In *Molecular Biology of Fungal Development*, pp. 29–58. Edited by H. D. Osiewacz. Boca Raton, FL: CRC Press.
- Beckett, A., Heath, I. & McLaughlin, D. J. (1974). *An Atlas of Fungal Ultrastructure*. London: Longman.
- Bentivoglio, M. & Mazzarello, P. (1998). The pathway to the cell and its organelles: one hundred years of the Golgi apparatus. *Endeavour* **22**, 101–105.
- Bevis, B. J., Hammond, A. T., Reinke, C. A. & Glick, B. S. (2002). *De novo* formation of transitional ER sites and Golgi structures in *Pichia pastoris*. *Nat Cell Biol* **4**, 750–756.
- Boevink, P., Oparka, K., Cruz, S. S., Martin, B., Betteridge, A. & Hawes, C. (1998). Stacks on tracks: the plant Golgi apparatus traffics on an actin. *Plant J* **15**, 441–447.
- Breakspear, A., Langford, K., Momany, M. & Assinder, S. S. (2007). CopA:GFP localizes to putative Golgi equivalents in *Aspergillus nidulans*. *FEMS Microbiol Lett* **277**, 90–97.
- Cole, L., Davies, D., Hyde, G. J. & Ashford, A. E. (2000). Brefeldin A affects growth, endoplasmic reticulum, Golgi bodies, tubular vacuole system, and secretory pathway in *Pisolithus tinctorius*. *Fungal Genet Biol* **29**, 95–106.
- daSilva, L. L. P., Snapp, E. L., Denecke, J., Lippincott-Schwartz, J., Hawes, C. & Brandizzi, F. (2004). Endoplasmic reticulum export sites and Golgi bodies behave as single mobile secretory units in plant cells. *Plant Cell* **16**, 1753–1771.
- Donaldson, J. G., Finazzi, D. & Klausner, R. D. (1992). Brefeldin A inhibits Golgi-membrane catalyzed exchange of guanine nucleotide onto ARF protein. *Nature* **360**, 350–352.
- Farquhar, M. G. & Palade, G. E. (1981). The Golgi apparatus (complex) – (1954–1981) from artifact to center stage. *J Cell Biol* **91**, 77s–103s.
- Farquhar, M. G. & Palade, G. E. (1998). The Golgi apparatus: 100 years of progress and controversy. *Trends Cell Biol* **8**, 2–10.
- Felenbok, B. (1991). The ethanol utilization regulon of *Aspergillus nidulans*: the *AlcA–AlcR* system as a tool for the expression of recombinant proteins. *J Biotechnol* **17**, 11–18.

- Fernández-Ábalos, J. M., Fox, F., Pitt, C., Wells, B. & Doonan, J. H. (1998).** Plant-adapted green fluorescent protein is a versatile vital reporter for gene expression, protein localization and mitosis in the filamentous fungus, *Aspergillus nidulans*. *Mol Microbiol* **27**, 121–130.
- Fischer, R. & Veith, D. (2007).** The role of microtubules and motors for polarized growth of filamentous fungi. In *Exploitation of Fungi: Symposium of the British Mycological Society held at the University of Manchester September 2005* (British Mycological Society Symposia no. 26), pp. 95–116. Edited by G. D. Robson, P. Van West & G. M. Gadd. Cambridge: Cambridge University Press.
- Harris, S. D., Morrell, J. L. & Hamer, J. E. (1994).** Identification and characterization of *Aspergillus nidulans* mutants defective in cytokinesis. *Genetics* **136**, 517–532.
- Hawes, C. & Satiat-Jeuemaitre, B. (2005).** The plant Golgi apparatus – going with the flow. *Biochim Biophys Acta* **1744**, 93–107.
- Heath, I. B. (1990).** The roles of actin in tip growth of fungi. *Int Rev Cytol* **123**, 95–127.
- Heath, I. B. (1995).** The cytoskeleton. In *The Growing Fungus*, 1st edn, pp. 99–134. Edited by N. A. R. Gow & G. M. Gadd. London: Chapman and Hall.
- Heath, I. B. & Kaminskyj, S. G. W. (1989).** The organization of tip-growth-related organelles and microtubules revealed by quantitative analysis of freeze-substituted oomycete hyphae. *J Cell Sci* **93**, 41–52.
- Helms, J. B. & Rothman, J. E. (1992).** Inhibition by brefeldin A of a Golgi membrane enzyme that catalyses exchange of guanine nucleotide bound to ARF. *Nature* **360**, 352–354.
- Hirt, H., Kogl, M. & Murbacher, T. (1990).** Evolutionary conservation of transcriptional machinery between yeast and plants as shown by the efficient expression from the CaMV 35S promoter and 35S terminator. *Curr Genet* **17**, 473–479.
- Hohmann-Marriott, M. F., Uchida, M., van de Meene, A. M. L., Garret, M., Hjelm, B. E., Kokoori, S. & Roberson, R. W. (2006).** Application of electron tomography to fungal ultrastructure studies. *New Phytol* **172**, 208–220.
- Hubbard, M. & Kaminskyj, S. G. W. (2007).** Growth rate of *Aspergillus nidulans* hyphae is independent of a prominent array of microtubules. *Mycol Prog* **6**, 179–189.
- Hubbard, M. (2007).** *In vivo study of the role of the cytoskeleton and fungal Golgi in hyphal tip growth of Aspergillus nidulans*. MSc thesis, University of Saskatchewan. Available at library2.usask.ca/theses/available/etd-05042007-171757
- Jackson, C. L. & Casanova, J. E. (2000).** Turning on ARF: the Sec7 family of guanine-nucleotide-exchange factors. *Trends Cell Biol* **10**, 60–67.
- Jefferson, R. A., Kavanagh, T. A. & Bevan, M. W. (1987).** GUS fusions:  $\beta$ -glucuronidase as a sensitive and versatile gene fusion marker in higher plants. *EMBO J* **6**, 3901–3908.
- Kaminskyj, S. G. W. (2001).** Fundamentals of growth, storage, genetics and microscopy of *Aspergillus nidulans*. *Fungal Genet Newsl* **48**, 25–31.
- Kaminskyj, S. G. W. & Boire, M. R. (2004).** Ultrastructure of the *Aspergillus nidulans* *hypA1* restrictive phenotype shows defects in endomembrane arrays and polarized wall deposition. *Can J Bot* **82**, 807–814.
- Kaminskyj, S. G. W. & Hamer, J. E. (1998).** *hyp* loci control cell pattern formation in the vegetative mycelium of *Aspergillus nidulans*. *Genetics* **148**, 669–680.
- Kaminskyj, S. G. W. & Heath, I. B. (1996).** Studies on *Saprolegnia ferax* suggest the general importance of the cytoplasm in determining hyphal morphology. *Mycologia* **88**, 20–37.
- Kaminskyj, S. G. W., Jackson, S. L. & Heath, I. B. (1992).** Fixation induces differential polarized translocations of organelles in hyphae of *Saprolegnia ferax*. *J Microsc* **167**, 153–168.
- Khalaj, V., Brookman, J. L. & Robson, G. D. (2001).** A study of the protein secretory pathway of *Aspergillus niger* using a glucoamylase–GFP fusion protein. *Fungal Genet Biol* **32**, 55–65.
- Kurtz, M. B., Heath, I. B., Marrinan, J., Dreikorn, S., Onishi, J. & Douglas, C. (1994).** Morphological effects of lipopeptides against *Aspergillus fumigatus* correlate with activities against (1,3)- $\beta$ -D-glucanase. *Antimicrob Agents Chemother* **38**, 1480–1489.
- Li, A., Altosaar, I., Heath, M. C. & Horgen, P. A. (1993).** Transient expression of the beta-glucuronidase gene delivered into urediniospores of *Uromyces appendiculatus* by particle bombardment. *Can J Plant Pathol* **15**, 1–6.
- Losev, E., Reinke, C. A., Jellen, J., Strongin, D. E., Bevis, B. J. & Glick, B. S. (2006).** Golgi maturation visualized in living yeast. *Nature* **441**, 1002–1006.
- Maruyama, J. & Kitamoto, K. (2007).** Differential distribution of the endoplasmic reticulum network in filamentous fungi. *FEMS Microbiol Lett* **272**, 1–7.
- Matheson, L. A., Hanton, S. L. & Brandizzi, F. (2006).** Traffic between the plant endoplasmic reticulum and Golgi apparatus: to the Golgi and beyond. *Curr Opin Plant Biol* **9**, 601–609.
- Matsuura-Tokita, K., Takeuchi, M., Ichihara, A., Mikuriya, K. & Nakano, A. (2006).** Live imaging of yeast Golgi cisternal maturation. *Nature* **441**, 1007–1010.
- McGoldrick, C. A., Gruver, C. & May, G. S. (1995).** *myoA* of *Aspergillus nidulans* encodes an essential myosin I required for secretion and polarized growth. *J Cell Biol* **128**, 577–587.
- Mogelsvang, S. & Howell, K. E. (2006).** Global approaches to study Golgi function. *Curr Opin Cell Biol* **18**, 438–443.
- Mogelsvang, S., Gomez-Ospina, N., Soderholm, J., Glick, B. S. & Staehelin, L. A. (2003).** Tomographic evidence for continuous turnover of Golgi cisternae in *Pichia pastoris*. *Mol Biol Cell* **14**, 2277–2291.
- Morris, N. R., Xiang, X. & Beckwith, S. M. (1995).** Nuclear migration advances in fungi. *Trends Cell Biol* **5**, 278–282.
- Munro, S. (1991).** Sequences within and adjacent to the transmembrane segment of  $\alpha$ -2,6-sialyltransferase specify Golgi retention. *EMBO J* **10**, 3577–3588.
- Odell, J. T. & Nagy, F. (1985).** Identification of DNA sequences required for activity of the cauliflower mosaic virus 35S promoter. *Nature* **313**, 810–812.
- Rida, P. C. G., Nishikawa, A., Won, G. Y. & Dean, N. (2006).** Yeast-to-hyphal transition triggers formin-dependent Golgi localization to the growing tip in *Candida albicans*. *Mol Biol Cell* **17**, 4364–4378.
- Rupeš, I., Mao, W. Z., Astrom, H. & Raudaskoski, M. (1995).** Effect of nocodazole and brefeldin-A on microtubule cytoskeleton and membrane organization in the homobasidiomycete *Schizophyllum commune*. *Protoplasts* **185**, 212–221.
- Schwientek, T., Lorenz, C. & Ernst, J. F. (1995).** Golgi localization in yeast is mediated by the membrane anchor region of rat liver sialyltransferase. *J Biol Chem* **270**, 5483–5489.
- Sharpless, K. E. & Harris, S. D. (2002).** Functional characterization and localization of the *Aspergillus nidulans* formin SEPA. *Mol Biol Cell* **13**, 469–479.
- Shi, X., Sha, Y. & Kaminskyj, S. (2004).** *Aspergillus nidulans hypA* regulates morphogenesis through the secretion pathway. *Fungal Genet Biol* **41**, 75–88.
- Suelmann, R. & Fischer, R. (2000a).** Mitochondrial movement and morphology depend on an intact actin cytoskeleton in *Aspergillus nidulans*. *Cell Motil Cytoskeleton* **45**, 42–50.

**Suelmann, R. & Fischer, R. (2000b).** Nuclear migration in fungi: different motors at work. *Res Microbiol* **151**, 247–254.

**Sun, L., Cai, H., Xu, W., Hu, Y. & Lin, Z. (2002).** CaMV 35S promoter directs  $\beta$ -glucuronidase expression in *Ganoderma lucidum* and *Pleurotus citrinopileatus*. *Mol Biotechnol* **20**, 239–244.

**Wee, E. G.-T., Sherrier, D. J., Prime, T. A. & Dupree, P. (1998).** Targeting of active sialyltransferase to the plant Golgi apparatus. *Plant Cell* **10**, 1759–1768.

**Whittaker, S. L., Lunness, P., Milward, K. J., Doonan, J. H. & Assinder, S. J. (1999).** *sodVIC* is an  $\alpha$ -COP-related gene which is essential for establishing and maintaining polarized growth in *Aspergillus nidulans*. *Fungal Genet Biol* **26**, 236–252.

**Xu, X., Mang, J., Li, X., Yu, M. & Ru, B. (2004).** Expression of human intestinal trefoil factor (hITF) in transgenic *Pleurotus ostreatus* and its ELISA assay. *Acta Microbiol Sin* **44**, 609–612.

---

Edited by: S. D. Harris